Nanoscale

Accepted Manuscript

This article can be cited before page numbers have been issued, to do this please use: H. Zhao, F. Liu, S. Wu, L. Yang, Y. Zhang and C. Li, *Nanoscale*, 2017, DOI: 10.1039/C6NR09300K.

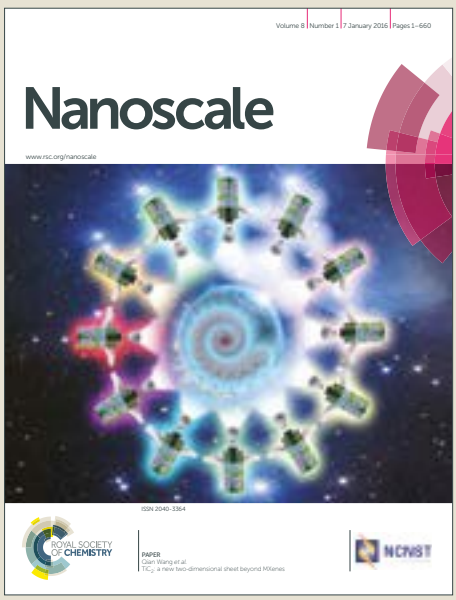

ROYAL SOCIETY OF CHEMISTRY

rsc.li/nanoscale

View Article Online
DOI: 10.1039/C6NR09300K

Ultrasensitive electrochemical detection of *Dicer1* 3'UTR for the fast analysis of alternative cleavage and polyadenylation

Hui Zhao[1,#], FengLiu[1, #], Shilian Wu[2], Long Yang[2,*], Ya-Ping Zhang [1, 3, *], Can-Peng Li[2,*]

[1]Laboratory for Conservation and Utilization of Bio-resource, Yunnan University, Kunming 650091, PR China.

[2]School of Chemical Science and Technology, Yunnan University, Kunming 650091, PR China.

[3]State Key Laboratory of Genetic Resources and Evolution, Kunming Institute of Zoology, Chinese Academy of Sciences, Kunming 650223, PR China.

[#]These authors contributed equally to this work.

[*]To whom should be correspondence. Fax or Tel: 86-871-65031119.

E-mail: long133109070@126.com (L. Yang); zhangyp@mail.kiz.ac.cn (Y.-P. Zhang); lcppp1974@sina.com(C.-P. Li).

View Article Online
DOI: 10.1039/C6NR09300K

Abstract: Alternative cleavage and polyadenylation (APA) is involved in several important biological processes in animals, e.g. cell growth and development, cancer progression. The increasing data show that cancer cells are inclined to produce mRNA isoforms with shortened 3'UTR undergoing APA. For example, the *Dicer1* isoform with shorter 3'untranslated region (3'UTR) was found to be overexpressed in some cancer cells, which may be used as a potential novel biomarkers for cancer prognostic. In the present work, a novel electrochemical biosensor for ultrasensitive determination of *Dicer1* was designed by using gold nanoparticles and p-sulfonated calix[6]arene functionalized reduced graphene oxide (Au@SCX6-rGO) as nanocarriers. The results showed that the expression of shorter 3'UTR (*Dicer1*-S) both in BT474 and SKBR3 were obviously higher those of longer*Dicer1* (*Dicer1*-L) by the constructed biosensor, which was well agree with the result analyzed by the RT-qPCR method. The detection ranges of *Dicer1*-S and *Dicer1*-L were 10^{-14}–10^{-9} M and 10^{-15}–10^{-10} M. The LODs were 3.5 and 0.53 fM. The specificity of the proposed biosensor was also very high. For the first time, the expressional analysis of different 3'UTR caused by APA was studied by an electrochemical method. Moreover, the use of macrocyclic host for constructing the electrochemical/biosensing platform is rarely reported. The proposed electrochemical sensing strategy is thus expected to provide new method for determination of novel biomarkers and novel method for fast and cheap analysis of APA.

Introduction

View Article Online
DOI: 10.1039/C6NR09300K

Cleavage and polyadenylation are prerequisite for mRNA maturation that includes the processes of cutting and adding an oligo (dA) tail to the 3' end of the nascent transcript.[1] Recent studies have demonstrated that 70%-79% of mammalian genes involve alternative cleavage and polyadenylation (APA), which can produce different mRNA isoforms.[2,3] Increasing evidences have shown that APA is involved in several biological processes in animals, e.g. cell growth and development, cancer progression.[4] For cleavage sites, the most widespread occurrence of APA is in the 3'-most exon and leads to variable 3'untranslated regions (UTRs) (**Scheme 1A**).[3] Of note, proliferating cells,[5] transformed cells,[6] and cancer cells[7-10] are inclined to produce mRNA isoforms with shortened 3'UTR, especially in proto-oncogenes. Tumors expressing shorter 3'UTRs tend to be more aggressive and to result in shorter patient survival during several cancer development.[9,10] Moreover, Singh and co-authors[8] have revealed that characteristic differences in 3'UTR can clinically distinct cancer subtypes, with at least 74% accuracy. Therefore, genes undergoing APA were suggested to be powerful novel biomarkers for cancer prognostic.[8,9] Dicer1 is a highly conserved RNase type III enzyme that plays an essential role in miRNA pathways.[11] The human *Dicer1* gene was reported to be three APA signals identified by 3'RACE.[6] Interestingly, the *Dicer1* isoform with shorter 3'UTR was found to overexpression in several cancer cells, such as lung cancer, colon cancer, and breast cancer.[6]

For expressional detection of mRNA isoforms by APA, several technologies including reverse transcription-quantitative polymerase chain reaction (RT-qPCR),

View Article Online
DOI: 10.1039/C6NR09300K

Northern blot, high throughput methods (microarrays and next generation sequencing) were often used in biological study. However, inherent disadvantages of these methods limit the clinical application. For instance, the accuracy of RT-qPCR depends on the design of PCR primer pairs and requires special equipment. Northern blot is low sensitivity. High throughput methods is time consumption, complex manipulations and high cost.[12,13]Due to its inherent simplicity, low cost, high sensitivity, and miniaturization, the electrochemical detection technique have attracted considerable attention.[13-15] In order to improve the amount of immobilization of biomolecules and enhance the sensitivity of the electrochemical detection method, various signal amplification strategies have been developed, such as rolling circle amplification, enzyme labeling amplification, and polymerase chain reaction.[16] Among these strategies, nanomaterial-based strategies have potential in realizing ultrasensitive biological detection due to the versatile properties of nanomaterials.[12] Based on this concept, many researchers choose some carbon materials such as carbon nanotubes,[17] carbon nanohorns,[18]graphene,[19-21] mesoporous carbons,[22,23] and fullerene[24]as efficient carriers. Among these carbon materials, graphene is one of the most promising materials that holds great promise for potential applications in many technological fields because of its high surface area, low cost, good biocompatibility, and high conductivity.[25]

In recent years, researchers are pushing ahead to develop the nanohybrids of macrocyclic hosts (e.g. cyclodextrins, calixarenes, cucurbiturils) and carbon materials (e.g. CNT, CNH, graphene) for various technological applications such as

View Article Online
DOI: 10.1039/C6NR09300K

electrochemical/optical sensing, bioimaging, drug delivery, and so on.[26] Calixarenes, recognized as the third class of macrocyclic host after crown ethers and cyclodextrins, which show high supramolecular recognition with various guest molecules.[27] Especially, the p-sulfonated calixarenes have been widely investigated for various applications due to their high water-solubility. It has been reported that the composites of calixarenes and carbon materials could be formed by π–π interactions and hydrogen interactions.[28, 29] If graphene are modified with water-soluble calixarenes, it is possible to obtain new functionalized materials that simultaneously possess the unique properties of graphene (superior conductivity and large specific surface area) and calixarenes (high supramolecular recognition capability) through combining their individual characteristics.

Herein, the p-sulfonated calix[6]arene functionalized reduced graphene oxide (SCX6-rGO) composite was prepared by a wet-chemical method in aqueous solution. Monodispersed gold nanoparticles (Au NPs) with a uniform size of ~5.0 nm were successfully anchored on the SCX6-rGO surface via an *in situ* growth approach. The proposed electrochemical biosensor for APA analysis approach is expected to be highly sensitive due to the use of the Au@SCX6-rGO composite as a nanocarrier, which was used to load large amount of redox-active probe MB based on the macrocyclic host SCX6 with excellent supramolecular recognition and enrichment capability. Thus, the proposed biosensor showed high sensitivity for quantitative APA assay. As illustrated in **Scheme 1B**, the proposed protocol for monitoring *Dicer1* involves the preparation of the Au@SCX6-rGO-MB-LP bioconjugate, the stepwise

View Article Online
DOI: 10.1039/C6NR09300K

modification of the proposed electrochemical biosensor. In addition, the procedure of the *Dicer1* detections by electrochemical biosensor and by RT-qPCR method was illustrated in **Fig. S1**.

Results and discussion

Detection specificity

As shown in **Scheme 1A**, Dicer1 gene can produce two mRNA isoforms with shorter 3'UTR (*Dicer1*-S) and longer 3'UTR (*Dicer1*-L) due to APA signals which were confirmed by Northern blot assay.[6] To ensure the specificity of PCR products, we performed in silico analysis using human genome database (http://genome.ucsc.edu), and then designed the qPCR primer pairs to amplify the 3'UTR of *Dicer1*-S and *Dicer1*-L. The results showed that all PCR assays produced single amplicons, indicated by the presence of single sharp amplification curves in qPCR reactions (**Fig. S2**). Furthermore, with sequencing, we confirmed the each qPCR reaction is specific (Data not shown). Correspondingly, the modified capture probes (CPs) were designed to hybridize the regions with in qPCR amplicons (**Scheme 1A**).

Characterization of Au@SCX6-rGO nanocomposite

As shown in **Fig. 1A**, the FTIR spectrum of rGO displays the stretching vibrations of –OH (3440 cm^{-1}), C–O (1200 cm^{-1}), and C–O/C–C (1090 cm^{-1}) due to a small amount of the remaining oxygen-containing functional groups. The C=C (1630 cm^{-1}) conjugation is observed in rGO. In the case of SCX6-rGO, the peaks of –OH (3440

View Article Online
DOI: 10.1039/C6NR09300K

cm^{-1}) and O–H bending vibrations (1401 cm^{-1}) enhanced obviously, which may be caused by the introduced –OH in SCX6. Besides, the typical peaks for $-SO_3^-$ at 1160 and 1040 cm^{-1} both appeared in the FTIR spectra of native SCX6 and the SCX6-rGO composite, implying that SCX6 molecules were grafted to the rGO. The prepared rGO and SCX6-rGO were characterized by TGA, as shown in **Fig. 1B**. For the rGO, the loss in mass (22 wt%) at a temperature of approximately 600 °C was due to the pyrolysis of the remaining oxygen-containing functional groups in rGO. The mass loss of the SCX6-rGO reached about 48 wt% when the temperature was 600 ^oC. To deduct the mass loss of rGO, the mass loss caused by the decomposition of SCX6 was 26 wt%. The zeta potential measurements of the RGO and SCX6-rGO were obtained as shown in **Figs. 1C and D**. The average zeta potentials of rGO and SCX6-rGO were –26.8 and –39.8 mV, respectively. The zeta potential of SCX6-rGO decreased approximately 13 mV compared with that of rGO, which was ascribed to the negative charge of $-SO_3^-$ in the SCX6 molecule. The zeta potential of SCX6-rGO was lower than –30 mV, suggesting that the colloidal stability of the SCX6-rGO dispersion was very high.[31] The AFM images of rGO and SCX6-rGO were also obtained. As shown in **Fig. 1E**, the thickness of the rGO through exfoliation revealed by the AFM image is 0.9±0.1 nm, which clearly demonstrates the single-layer feature of rGO, according to the previous literature.[28] However, a remarkable increase of thickness to 1.4±0.1 nm (**Fig. 1F**) is observed in the AFM images after the introduction of SCX6 into rGO. Comparing the thickness of rGO and SCX6-rGO reveals that the thickness increase is a result of the chemical derivatization by the SCX6 on the rGO. Therefore, all these

View Article Online
DOI: 10.1039/C6NR09300K

results demonstrated that the SCX6 had successfully grafted on the rGO.

The morphology and microstructure of theAu@SCX6-rGO was investigated by using TEM. **Fig. 2A**shows the TEM image of theAu@SCX6-rGO material. The Au NPs with a uniform size of ~5.0 nm were fairly well monodispersed on the surface of SCX6-rGO. The EDX analysis of Au@SCX6-rGOwas illustrated in **Fig. 2B**. It can be clearly noticed that the Au, C, and O elements were presented in the Au@SCX6-rGOcomposite. On the basis of the quantitative analysis of the EDX data, the weight percentages of C, O, and Au in the composite are estimated to be 60.26, 34.88, and 4.86%, respectively. XPS analysis was used to determine the electronic structure and compositions ofAu@SCX6-rGO. As shown in **Fig. 2C**, the survey spectrum confirms the presence of Au, C, and O in the composite, which is in agreement with EDX result. The Na signal is attributed to residual NaOH. The high-resolution spectrum of Au 4f in **Fig. 2D** obviously shows that the peaks centered at 83.5 and 87.2 can be assigned to Au $4f_{7/2}$ and Au $4f_{5/2}$ peaks, respectively, confirming the presence of Au in the composites. **Fig. 2F** is the C 1s spectrum, which reveals that there are three components of carbon bond, namely sp^2 C (284.5 eV), sp^3 C (285.3 eV), C−O (286.5 eV), C=O (287.8 eV), and O−C=O (288.8 eV) are presented in the composites. Moreover, compared with the C 1s spectra of GO (**Fig. 2E**), the intensities of the C=C/C–C peaks in Au@SCX6-rGO became predominant, while the intensities of all C1s peaks of the carbon binding to oxygen (C–O, C=O, and O–C=O) decreased significantly, which also demonstrates the removal of mostly the oxygen-containing functional groups after the reduction and formation of rGO.

View Article Online
DOI: 10.1039/C6NR09300K

Feasibility of the *Dicer1*-S and *Dicer1*-L biosensors

The feasibility of the proposed HT/CP-S/Au/GCE biosensor was explored with different modified surfaces by DPV responses for 10^{-11} M *Dicer1*-S. As can be seen from **Fig. 3A**, almost no detectable electrochemical signal is observed for the biosensor hybridized with *Dicer1-S* (curve a) due to the absence of the redox mediator MB. The hybridization of the Au@SCX6-RGO-MB-LP-S bioconjugate and AP-S caused an increase in current response because of the formation of the CP-S-*Dicer1*-S complex and attachment of Au@SCX6-RGO-MB-LP-S bioconjugate which containing redox-active probe MB (curve b). These results clearly demonstrated that the proposed electrochemical method is feasible for the detection of the *Dicer1*-S. The feasibility of the HT/CP-L/Au/GCE was similar to that of the HT/CP-S/Au/GCE biosensor.

EIS characterization of *Dicer1*-S and *Dicer1*-L biosensors

EIS which can indicate the change of surface area, resistance and carried charge could provide additional information about electrode surface modification. Thus, the assembly process of modified electrode could be monitored using EIS techniques, which has been proven to be one of the most powerful tools for characterizing the interface properties of the modified biosensors. The impedance spectra include a semicircle portion and a linear portion. The semicircle portion at higher frequencies corresponds to the electron-transfer limited process, and the linear portion at lower

View Article Online
DOI: 10.1039/C6NR09300K

frequencies represents the diffusion-limited process. The semicircle diameter equals the electron-transfer resistance. **Fig. 3B** shows the Nyquist diagrams of EIS upon the stepwise modification process. After electrodeposition of Au NPs, it was observed that the EIS of Au modified electrode decreased obviously compared with the bare GCE, indicating that the high conductivity of Au NPs can facilitate electron transfer. However, upon immobilization of CP-S on the modified electrode, the resistance increased obviously, which suggested that the CP-S was successfully immobilized on the surface and formed an additional barrier and hindered the tunnel of electron shuttle between the redox probe and the electrode. Non-conductive HT as the blocking agent made the resistance increased again. Then, the incubation of *Dicer1*-S (10^{-10} M) led to further increase of the resistance, attributing to the formation of CP-S-*Dicer1*-S complex on electrode surface which increased steric hindrance and blocked electron transfer. At last, when the Au@SCX6-RGO-MB-LP-S bioconjugate and AP-S hybridized with *Dicer1*-S (curve g), the resistance has no obvious change, indicating that the synthesized Au@SCX6-RGO-MB-LP-S bioconjugate possess high conductivity and good electron transfer efficiency, although the nucleotide sequence adsorption layer acted as barrier to the interfacial electron transfer. The EIS results demonstrated the successful fabrication of the electrochemical biosensor. The EIS characterization of the *Dicer1*-L biosensor was similar to that of *Dicer1*-S. The CV characterizations of the modified electrodes were also obtained as shown in **Fig. S3**.

Calibration curve of the *Dicer1*-S and *Dicer1*-L biosensor

View Article Online
DOI: 10.1039/C6NR09300K

The analytical performance of the proposed *Dicer1*-S biosensor incubated with different concentrations of *Dicer1*-S was assessed using DPV in 0.1 M pH 7.0 PBS. From **Fig. 3C**, it can be seen that DPV peaks exhibited clear dependence on the concentrations of target *Dicer1*-S because elevated *Dicer1*-S concentrations from 10^{-14} to 10^{-9} M led to increases in current responses, which suggested the hybridization of more Au@SCX6-RGO-MB-LP-S bioconjugate, AP-S, and abundant immobilization of the redox mediator MB on the electrode surface. As shown in **Fig. 3D**, the resulting calibration plot displayed a good linear relationship between the current response and the logarithm of *Dicer1*-S concentration ranging from 10^{-14} to 10^{-9} M, and a detection limit of 3.5 fM could be estimated using the 3σ rule. The detection limit (LOD) was calculated by using the equation: LOD=3S/b, where S is the standard deviation (SD) of the blank solution, b is the slope of the analytical curve. The corresponding regression equation was I (μA) = –0.27 logC – 3.88 with a correlation coefficient of 0.987. The proposed *Dicer1*-L biosensor incubated with different concentrations of *Dicer1*-L was investigated using DPV in 0.1 M pH 7.0 PBS. As shown in **Fig. 3E**, the DPV currents increased with the increasing of the *Dicer1*-L concentrations from 10^{-15} to 10^{-10} M. The resulting calibration plot (**Fig. 3F**) also illustrated a good linear relationship between the current response and the logarithm of *Dicer1*-L concentration ranging from 10^{-15} to 10^{-10} M, and a detection limit of 0.53 fM could be estimated using the 3σ rule. The corresponding regression equation was I (μA) = –0.10 logC – 1.57 with a correlation coefficient of 0.982. Compared with some previous published papers (**Table 1**), the proposed *Dicer1*

View Article Online
DOI: 10.1039/C6NR09300K

biosensor exhibited high sensitivity, which was attributed to the superior conductivities of rGO and Au NPs, the large specific surface area of rGO, and high loading of redox-active probe MB based on the macrocyclic host SCX6 which possesses excellent supramolecular recognition and enrichment capability.

Detection of *Dicer1*-S and *Dicer1*-L and analysis of APA in breast cancer cells

In recent years, the detection of RNA in cells has been studied widely. [42-45] However, the analysis of APA is rarely reported. To examine the selectivity of our proposed biosensor, we performed a comparison study on mismatch targets and perfect complementary target. As shown in **Fig. 4A**, the 1MT-S, 2MT-S, 2MT-L, and NC resulted very small response, while the BT474-S, BT474-L, SKBR3-S, and SKBR3-L significantly increased the current. This revealed the high specificity of the proposed electrochemical biosensor.

The reproducibility and stability of the biosensor were also studied. The reproducibility of the biosensor was examined by six equally proposed biosensors incubated with the same concentration *Dicer1*-S (10^{-10} M) or *Dicer1*-L (10^{-10} M). The six electrodes exhibited the similar responses and a relative standard deviation (RSD) of 1.8% for *Dicer1*-S and 4.3% for *Dicer1*-Lwas obtained, indicating satisfying reproducibility. The long-term storage assay was used to examine the stability of the proposed biosensor. The long-term stability experiment was carried out intermittently (every 5 days). When the biosensor was not in use, it was stored in a refrigerator at 4 ^{o}C. Over 94.5% and 86.6% of initial response remained after storage of 15 and 30

View Article Online
DOI: 10.1039/C6NR09300K

days, respectively.

To demonstrate the applicability of our biosensor for detecting different 3'UTR of *Dicer1* due to APA, we tested real samples from two human breast cancer cell lines (BT474 and SKBR3). Total RNA was extracted and quantified for the detection of *Dicer1*-S and *Dicer1*-L. The concentrations of *Dicer1*-S and *Dicer1*-L were detected by the proposed electrochemical biosensor as showed in **Fig. 4B**. The expression of *Dicer1*-S both in BT474 and SKBR3 was obviously higher that of *Dicer1*-L. To validate the detection by electrochemical biosensor, we used RT-qPCR method, the most used technology in biological research, to provide a quantitative comparison (**Fig. 4C**). The results showed that the expression of *Dicer1*-S and *Dicer1*-L exhibits similar high-low patterns between the two detecting methods. Previous studies have shown that the lower expressional ratio between long isoform and short isoform (LSR) has been found in cancer cell lines, and correlates with poor prognosis in breast and lung cancer.[6, 10] The 3'UTR plays a curial role in regulating mRNA expression level *via* providing microRNA (miRNA) binding sites. Intelligibly, as shorten 3'UTR has fewer *cis*-regulatory elements, such as miRNA binding sites, the oncogenes with shorten 3'UTR express more proteins by escaping miRNA control. Interestingly, the expression levels of *Dicer1*-S were significantly higher than those of *Dicer1*-L both in BT474 and SKBR3 cells. For example, the LSR between *Dicer1*-L and *Dicer1*-S was 0.236 and 0.301 detected by biosensor in BT474 cells and SKBR3 cells, respectively. The results of LSR are in good agreement with those obtained by RT-qPCR on the same samples (0.227 and 0.267, respectively). Moreover, the detection limit of our

View Article Online
DOI: 10.1039/C6NR09300K

method is much lower than those achieved by conventional or modified biochemical techniques, such as fluorescent correlation spectroscopy[32] quantum dot-based miRNA profiling microarray assay[33] and Northern blotting assay.[34, 35]

To the best of our knowledge, this is the first report on expressional detection of different 3'UTR due to APA. As an important fact, the RT-qPCR results have not units and cannot provide precise quantitative detection. However, the constructed electrochemical biosensor can provide the credible and actual quantitative analysis in real samples. Furthermore, it is worthy to note that this electrochemical method is simpler, faster, and cheaper than the conventional methods, such as RT-qPCR, Northern blot, and high throughput method. Therefore, this technology can be used in APA analysis of animals' biological processes or diagnostics at the point of care.

Materials and methods

Chemicals and materials

Graphite oxide (GO) was purchased from Nanjing XFNANO Materials Tech Co., Ltd. (Nanjing, China). p-Sulfonated calix[6]arene (SCX6) was obtained from Tokyo Chemical Industry Co., Ltd. (Tokyo, Japan). $HAuCl_4$ and tris(2-carboxyethyl) phosphine hydrochloride (TCEP) were purchased from Sigma Chemical Co. (St. Louis, MO, USA). All other reagents were of analytical grade. All aqueous solutions were prepared with deionized water (18 MΩ cm).

The buffers and solutions involved in this work were as follows: DNA immobilization buffer (I-buffer; 10 mM Tris–HCl containing 1 mM EDTA, 300 mM

View Article Online
DOI: 10.1039/C6NR09300K

NaCl and 10 mM TCEP, pH 7.4), DNA hybridization buffer (H-buffer; 10 mM Tris–HCl containing 1 mM EDTA, 0.3 M NaCl and 1 mM $MgCl_2$, pH 7.4), and electrochemical impedance spectroscopy testing buffer (E-buffer; 0.1 M PBS containing 2.0 mM $K_4[Fe(CN)_6]/K_3[Fe(CN)_6]$ and 0.1 M KCl, pH 7.4).

Sample preparation

Breast cancer cell lines BT474 and SKBR3 were cultured described as previous report (Liu et al., 2005). Total RNA extraction including DNase treatment with RNase-free DNase I set (TianGen) was carried out using the RNeasy Mini Kit (Qiagen) according to the manufacturer's instructions. Extracted RNAs were quantified by NanoDrop 2000 Spectrophotometer (Thermo Fisher Scientific), and the absorbance ratio at 260/280 and 260/230 were measured to assure RNA purity. Total RNA (2 μg) was reverse-transcribed using the PrimeScript RT reagent Kit (Takara Biotechnology) according to the manufacturer's instructions.

Primer and probes design

The sequence of *Dicer1* was downloaded from NCBI database (GenBank accession No. NG_016311.1) and definite the APA sites according to previous report (Mayr et al., 2009). Real-time PCR (qPCR) primer pairs were designed using primer Express 3.0 software. Each primer set and capture probes were confirmed to be specific to their targeting regions with no homology to other sequences at UCSC's human genome browser (http://genome.ucsc.edu). PCR products were further cloned into

View Article Online
DOI: 10.1039/C6NR09300K

PMD18-T vector (Takara Biotechnology) and sequenced for verification using an ABI PRISM 3730 DNA sequencer (Applied Biosystems). The sequences of primers and probes are listed in **Table S1**.

Preparation of Au@SCX6-rGO

The SCX6-rGO composite was prepared according to our previous method.[30] In a typical experiment, 20 mL of 0.5 mg mL^{-1} GO aqueous suspension was mixed with 20 mL of 1.0 mg mL^{-1} SCX6 aqueous solution. Then, the pH of the mixture was adjusted to 12.0 using 1.0 M NaOH. Then it was transferred to a round bottom flask and stirred at 90 ^{o}C in an oil bath for 4 h. After cooling to room temperature, the resulting stable black dispersion was centrifuged at 16,000 rpm and washed with DW for three times. Finally, the resulting SCX6-rGO material was obtained by freeze-drying. TheAu@SCX6-rGO was synthesized according to a published paper [41] with some modifications, 10.0 mg SCX6-rGOwere dispersed into 10.0 mL of DW *via* sonication. Then 0.25 mL of 10 mM $HAuCl_4$ aqueous solution was added to the SCX6-rGO suspension dropwise and stirred at room temperature for 1 h. After centrifuging and washing with DW for three times,the resultingAu@SCX6-rGO was obtained by freeze-drying.

Materials characterizations

The morphologies of the prepared Au@SCX6-rGO and related samples were characterized by a Nanoscope III Atomic force microscopy (AFM) and a JEM 2100

View Article Online
DOI: 10.1039/C6NR09300K

transmission electron microscopy (TEM, Japan) equipped with an energy dispersive X-ray spectrometry (EDX). Fourier transform infrared (FT-IR) study (wavenumber) was performed overthe range of 4000–400 $cm^{-1}$by a Thermo Fisher SCIENTIFIC Nicolet IS10 (Thermo Fisher, USA) FT-IR impact 410 spectrophotometer using KBr pellets. Thermogravimetric analysis (TGA) was carried out on a Q50 TGA (TA Instruments, New Castle, DE, USA), ata heating rate of 10^{o}C/min from 35 to 800 ^{o}C in nitrogen. X-ray photoelectron spectroscopy (XPS) measurements were performed with Al Ka X-ray radiation as the X-ray source for excitation, which were carried out on an ESCALAB-MKII spectrometer (VG Co., United Kingdom). A Malvern Zetasizer Nano series was used for the zeta potential measurements.

Preparation of Au@SCX6-rGO-MB-LP-S and Au@SCX6-rGO-MB-LP-L bioconjugates

According to the method of Xu et al.,[12] the MB and LP were assembled on the Au@SCX6-rGO material. Initially, 2.0 mL of 1.0 mg mL^{-1} MB aqueous solutions were added into 2.0 mL of 1.0 mg mL^{-1} Au@SCX6-rGO aqueous solutions and stirred at room temperature for 12 h. After excess MB was removed by centrifugation and washing with DW three times, the resulting Au@SCX6-rGO-MB nanocomposite was re-dispersed in 2.0 mL of 0.1 M pH 7.0 PBS and stored at 4 ^{o}C before use. Secondly, 10 μL of 100 μM LP-S was added dropwise into the 80 μL of the Au@SCX6-rGO-MB mixture under continuous stirring gently at 4 ^{o}C for 12 h. Finally, the Au@SCX6-rGO-MB-LP-S bioconjugate was obtained by further

View Article Online
DOI: 10.1039/C6NR09300K

centrifugation and re-dispersed in 100 μL pH 7.0 PBS for further use. All the above experiments were performed at 4 ºC. The Au@SCX6-rGO-MB-LP-L bioconjugate was also obtained by using the same procedure.

Fabrication of the *Dicer1*-S and *Dicer1*-L biosensors

Prior to the preparation procedure, glassy carbon electrode (GCE, 3 mm in diameter) was polished with 0.3 and 0.05 μm Al_2O_3 powder respectively and subsequently sonicated in ethanol and DW to remove the physically adsorbed substance and dried at in air. Then Au NPs were electrodeposited on the cleaned and dried GCE surface in 10 mM $HAuCl_4$ aqueous solution under the potential –0.2 V for 200 s. Subsequently, the Au modified electrode was submerged into a solution of 10 μM CP-S or CP-L at 4 ^oC for 12 h to yield CP-S/Au/GCE or CP-L/Au/GCE. Finally, to block possible remaining active sites and eliminate the risk of nonspecific binding, 10 μL of 1.0 mM HT was coated on the electrode and incubated at room temperature for 30 min. Ultimately, the HT/CP-S/Au/GCE or HT/CP-L/Au/GCE was obtained and stored at 4 ºC when not in use. After each modification step, the modified electrode was cleaned with 0.1 M pH 7.0 PBS to remove the physically absorbed species.

Electrochemical measurements

Differential pulse voltammetry (DPV), cyclic voltammetry (CV) and electrochemical impedance spectroscopy (EIS) experiments were performed with a CHI 660E Electrochemical Workstation from Shanghai Chenhua Instrument (Shanghai, China)

View Article Online
DOI: 10.1039/C6NR09300K

and conducted using a three-electrode system, with the modified GCE as working electrode, a platinum wire as the counter electrode, a saturated calomel electrode as the reference electrode. All the measurements were carried out at room temperature. The biosensor was first incubated with 10 μL of H-buffer containing target DNA (*Dicer1*-S or *Dicer1*-L) with various concentrations for 1 h at room temperature, then incubated with a mixture of 10 μL of H-buffer containing Au@SCX6-rGO-MB-LP-S or Au@SCX6-rGO-MB-LP-L bioconjugate and 10 μL of 10 μM AP-S or 10 μL of 10 μM AP-L for another 1.0 h at room temperature. Each assembling procedure was followed by a careful rinse to remove excess materials in the electrode surface. DPV response was recorded in 0.1 M pH 7.0 PBS with a potential range of 0.1 to –0.6 V, modulation amplitude of 0.05 V, pulse width of 0.05 s. Additionally, electrochemical characterization of the biosensor using EIS and CV investigations were performed in 0.1 M pH 7.0 PBS containing 2 mM $[Fe(CN)_6]^{3-/4-}$ and 0.1 M KCl. EIS was tested at the potential of 0.1 V in the frequency range of 10^{-1} ~ 10^5 Hz with an amplitude of 5 mV.

RT-qPCR and expression analysis

RT-qPCR reactions were conducted in a 96-well plate using ABI PRISM 7500 Real-Time system (Applied Biosystems). Each reaction was performed in triplicate and in a 20 μL volume containing 1× SYBR Premix Ex Taq II (Takara Biotechnology), 50 nM of each primer and 1.0 μL cDNA. The cycling conditions were as follows: 95 °C for 10 sec, followed by 40 cycles of 95 °C for 5 sec, and 60 °C for 31 sec. PCR

View Article Online
DOI: 10.1039/C6NR09300K

reaction specificity was confirmed by DNA melting curve analysis and gel electrophoresis of product. The relative expression of *Dicer1*-L and *Dicer1*-S isoforms was calculated using ACTB as an endogenous control gene by the $2^{-\Delta\Delta Ct}$ method.

Conclusions

In summary, an electrochemical biosensor for determination of *Dicer1*and analysis of APA based on Au@SCX6-rGO as nanocarriers was developed. The expression of *Dicer1*-S both in BT474 and SKBR3 were higher than those of *Dicer1*-L demonstrated by the proposed biosensor, which was well agree with the result analyzed by the RT-qPCR method. The employment of Au@SCX6-rGO as nanocarriers led to attachment of large amounts of redox-active probe MB on the electrode surface. The macrocyclic host SCX6 possesses excellent supramolecular recognition and enrichment capability. Due to the superior conductivities of rGO and Au NPs, the large specific surface area of rGO, and high loading of redox-active probe MB, the electrochemical method showed high sensitivity. In view of these advantages, the proposed electrochemical sensing strategy is thus expected to provide new method for determination of biomarkers and method for fast and cheap analysis of alternative cleavage and polyadenylation.

Acknowledgements

This work was financiallysupported by the National Natural Science Foundation of

View Article Online
DOI: 10.1039/C6NR09300K

China (21565029, 31260032, 31460038) and the Program for Excellent Young Talents (WX069051), Yunnan University.

Conflict of interest statement. None declared.

References

1. D. F. Colgan and J. L. Manley, *Genes Dev.*, 1997, **11**, 2755–2766.
2. A. Derti, P. Garrett-Engele, K. D. Macisaac, R. C. Stevens, S. Sriram, R. Chen, C. A. Rohl, J. M. Johnson and T. Babak, *Genome Res.*, 2012, **22**, 1173–1183.
3. M. Hoque, Z. Ji, D. Zheng, W. Luo, W. Li, B. You, J. Y. Park, G. Yehia, B. Tian, *Nat. Methods*, 2013, **10**, 133–139.
4. B. Tian and J. L. Manley, *Trends Biochem Sci.*, 2013, **38**, 312–320.
5. R. Sandberg, J. R. Neilson, A. Sarma, P. A. Sharp and C. B. Burge, *Science*, 2008, **320**, 1643–1647.
6. C. Mayr and D. P. Bartel, *Cell*, 2009, **138**, 673–684.
7. Y. Fu, Y. Sun, Y. Li, J. Li, X. Rao, C. Chen and A. Xu, *Genome Res.*, 2011, **21**, 741–747.
8. P. Singh, T.L. Alley, S.M. Wright, S. Kamdar, W. Schott, R.Y. Wilpan, K. D. Mills and J. H. Graber, *Cancer Res.*, 2009, **69**, 9422–9430.
9. A. R. Morris, A. Bos, B. Diosdado, K. Rooijers, R. Elkon, A. S. Bolijn, B. Carvalho, G. A. Meijer and R. Agami, *Clin. Cancer Res.*, 2012, **18**, 5256–5266.
10. A. Lembo, F. Di Cunto and P. Provero, *PLoS ONE*, 2012, **7**, e31129.
11. W. D. Foulkes, J. R. Priest and T. F. Duchaine, *Nat. Rev. Cancer*, 2014, **14**,

View Article Online
DOI: 10.1039/C6NR09300K

662–672.

12. W. Xu, Y. Wu, H. Yi, L. Bai, Y. Chai and R. Yuan, *Chem. Commun.*, 2014, **50**, 1451–1453.
13. F. Liu, G. M. Xiang, D. N. Jiang, L. Q. Zhang, X. M. Chen, L. L. Liu, F. K. Luo, Y. Li, C. Liu and X.Y. Pu, *Biosens. Bioelectron.*, 2015, **74**, 214–221.
14. L. Yang, S. M. Fan, G. G. Deng, Y. C. Li, X. Ran, H. Zhao and C.-P. Li, *Biosens. Bioelectron.*, 2015, **68**, 617–625.
15. L. Yang, X. Ran, L. Cai, Y. C. Li, H. Zhao and C.-P. Li, *Biosens. Bioelectron.*, 2016, **83**, 347–352.
16. W. Xu, S. Xue, H. Yi, P. Jing, Y. Chai and R. Yuan, *Chem. Commun.*, 2015, **51**, 1472–1474.
17. R. Das, S. Upadhyay, M. K. Sharma, M. Shaik, V. K. Rao and D. N. Srivastav, *RSC Adv.*, 2015, **5**, 48147–48153.
18. F. Yang, J. Han, Y. Zhuo, Z. Yang, Y. Chai and R. Yuan, *Biosens. Bioelectron.*, 2014, **55**, 360–365.
19. G. Sun, J. Lu, S. Ge, X. Song, J. Yu, M. Yan and J. Huang, *Anal. Chim. Acta*, 2013, **775**, 85–92.
20. K. Shang, X. Wang, B. Sun, Z. Cheng and S. Ai, *Biosens. Bioelectron.*, 2013, **45**, 40–45.
21. R. Zhang, B. Pan, H. Wang, J. Dan, C. Hong and H. Li, *RSC Adv.*, 2015, **5**, 38176–38182.
22. H. Fan, Y. Zhang, D. Wu, H. Ma, X. Li, Y. Li, H. Wang, H. Li, B. Du and Q. Wei,

View Article Online
DOI: 10.1039/C6NR09300K

Anal. Chim. Acta, 2013, **770**, 62–67.

23. D. Wu, A. Guo, Z. Guo, L. Xie, Q. Wei and B. Du, *Biosens. Bioelectron.*, 2014, **54**, 634–639.
24. H. Wang, J. Zhang, Y. Yuan, Y. Chai and R. Yuan, *RSC Adv.*, 2015, **5**, 58019–58023.
25. M. J. Allen, V. C. Tung and R. B. Kaner, *Chem. Rev.*, 2010, **110**, 132–145.
26. H.Z.Ye, L. Yang.G.F. Zhao.Y.Q. Zhang.X. Ran.S.L. Wu, S. Zou, X.G. Xie, H. Zhao and C.-P. Li, *RSC Adv.*, 2016, **6**, 79350–79360.
27. X. W. Mao, H. Y. Zhao, L. Luo, D. M. Tian and H. B. Li, *J. Mater. Chem. C*, 2015, **3**, 1325–1329.
28. X. W. Mao, D. M. Tian and H. B. Li, *Chem. Commun.*, 2012, **48**, 4851–4853.
29. J. Zhou, M. Chen and G. W. Diao, *ACS Appl. Mater. Interfaces*, 2013, **5**, 828–836.
30. L. Yang, H. Zhao, Y.C. Li, X. Ran, G. G. Deng, X.G. Xie and C.-P. Li, *ACS Appl. Mater. Interfaces*, 2015, **7**, 26557−26565.
31. G. T. Fu, L. Tao, M. Zhang, Y. Chen, Y. W. Tang, J. Lin and T. H. Lu, *Nanoscale*, 2013, **5**, 8007–8014.
32. H. S. Yin, Y. L. Zhou, H. X. Zhang, X. M. Meng and S. Y. Ai, *Biosens. Bioelectron.*, 2012, **33**, 247–253.
33. L. A. Neely, S. Patel, J. Garver, M. Gallo, M. Hackett, S. McLaughlin, M. Nadel, J. Harris, S. Gullans and J. Rooke, *Nature Methods*,2006, **3**, 41–46.
34. R. Q. Liang, W. Li, Y. Li, C. Y. Tan, J. X. Li, Y. X. Jin and K. C. Ruan, *Nucleic*

View Article Online
DOI: 10.1039/C6NR09300K

Acids Res., 2005, **33**, e17.

35. S. H. Ramkissoon, L. A. Mainwaring, E. M. Sloand, N. S. Young and S. Kajigaya, *Mol. Cell. Probes*, 2006, **20**, 1−4.
36. A. Valoczi, C. Hornyik, N. Varga, J. Burgyan, S. Kauppinen and Z. Havelda, *Nucleic Acids Res.*, 2004, **32**, e175.
37. W. Shen, H. M. Deng, Y. Q. Ren and Z. Q. Gao, *Biosens. Bioelectron.*, 2013, **44**, 171–176.
38. J. X. Wang, X. Y. Yi, H. L. Tang, H. X. Han, M. H. Wu and F. M. Zhou, *Anal. Chem.*, 2012, **15**, 6400–6406.
39. M. Bartosik, R. Hrstka, E. Palecek and B. Vojtesek, *Anal Chim Acta*, 2014, **813**, 35–40.
40. P. Miao, B. Wang, Z. Yu, J. Zhao and Y. Tang, *Biosens Bioelectron.*, 2015, **63**, 365–370.
41. H. J. Yin, H. J. Tang, D. Wang, Y. Gao and Z. Y. Tang, *ACS Nano*, 2012, **6**, 8288–8297.
42. S. Li, L. G. Xu, W. Ma, X. L. Wu, M. Z. Sun, H. Kuang, L. B. Wang, N. A. Kotov, and C. L. Xu, *J. Am. Chem. Soc.*, 2016, **138**, 306–312.
43. M. Z. Sun,L. G. Xu,P. Fu,X. L. Wu,H. Kuang,L. Q. Liu,C. L. Xu, *Adv. Funct. Mater.*, 2016, **26**, 7352–7358.
44. L. G. Xu,S. Zhao,W. Ma,X. L. Wu,S. Li,H. Kuang,L. B. Wang,C. L. Xu, *Adv. Funct. Mater.*, 2016, **26**, 1602–1608.
45. X. L. Zhao,L. G. Xu,M. Z. Sun,W. Ma,X. L. Wu,H. Kuang,L. B. Wang,C. L. Xu,

View Article Online
DOI: 10.1039/C6NR09300K

Small, 2016, **12**, 4662–4668.

Figure legends

Scheme 1 (A)Schematic illustration of *Dicer1* isoforms due to APA and capture probes for electrochemical biosensor. The *Dicer1* gene produces the *Dicer1*-S and *Dicer1*-L isoforms cleaved by proximal polyadenylation site (pA) and distal pA, respectively. Black boxes show protein coding region (CDS); grey boxes represents 3' untranslated regions (3'UTR), and AAAAAA shows the poly(A) tail. Green and blue lines represent the capture probes (CPs) to hybridize the shorter 3'UTR and longer 3'UTR of *Dicer1*, respectively. (B)Schematic diagram for the stepwise assembly procedure of the electrochemical biosensor and signal conversion strategy. CP is CP-S or CP-L; target DNA is *Dicer1*-S or *Dicer1*-L; LP is LP-S or LP-L; AP is AP-S or AP-L.

Fig. 1 FTIR spectra of rGO, rGO@SCX6, and SCX6 (A); TGA curves of rGO and rGO@SCX6 (B); Zeta potentials of rGO (C) and rGO@SCX6 (D); AFM images of rGO (E) and rGO@SCX6 (F).

Fig. 2 TEM image of Au@SCX6-rGO (A); EDX analysis of Au@SCX6-rGO (B); XPS survey spectrum of Au@SCX6-rGO (C); the narrow spectra of Au 4f (D) and C 1s (F); the narrow spectrum of C 1s of GO (E).

View Article Online
DOI: 10.1039/C6NR09300K

Fig. 3 (A) DPV curves of the proposed *Dicer1*-S biosensor incubated with (a) 10^{-11} M *Dicer1*-S and (b) a mixture of Au@SCX6-RGO-MB-LP-S bioconjugate and AP-S in 0.1 M pH 7.0 PBS. DPV measurements were carried out by scanning the potential from 0.0 to –0.5 V with an amplitude of 0.05 V, a pulse width of 0.05 s, and a sample width of 0.0167s. (B) EIS characterization of different modified electrode: (a) bare GCE; (b) Au/GCE; (c) CP-S/Au/GCE; (d) HT/CP-S/Au/GCE; (e) *Dicer1*-S/HT/CP-S/Au/GCE; (f) Au@SCX6-RGO-MB-LP-S bioconjugate + AP-S/*Dicer1*-S/HT/CP-S/Au/GCE in 0.1 M pH 7.0 PBS containing 2.0 mM $[Fe(CN)_6]^{3-/4-}$ and 0.1 M KCl. EIS was recorded in the frequency range of $10^{-1} \sim 10^{5}$ Hz with an amplitude of 5 mV. (C) DPV curves for different concentrations of *Dicer1*-S for the proposed HT/CP-S/Au/GCE biosensor in 0.1 M pH 7.0 PBS. (D) The resulting calibration plot for log[*Dicer1*-S] *vs*. DPV response in the range of 10^{-14} to 10^{-9} M. Error bars: SD, *n*= 6. (E) DPV curves for different concentrations of *Dicer1*-L for the proposed HT/CP-L/Au/GCE biosensor in 0.1 M pH 7.0 PBS. (F) The resulting calibration plot for log[*Dicer1*-L] *vs*. DPV response in the range of 10^{-15} to 10^{-10} M. Error bars: SD, *n*= 6.

Fig. 4 (A) Selectivity of the biosensor. The comparison of APA determination using two methods. The determination of the *Dicer1*-S and *Dicer1*-L isoforms was performed using electrochemical biosensor (B) and the traditional RT-qPCR method (C) in BT474 and SKBR3 cell lines. Bars indicate the SD evaluated from three replicates. ** indicates and P<0.01. S: *Dicer1*-S; L: *Dicer1*-L.

View Article Online
DOI: 10.1039/C6NR09300K

Figures:

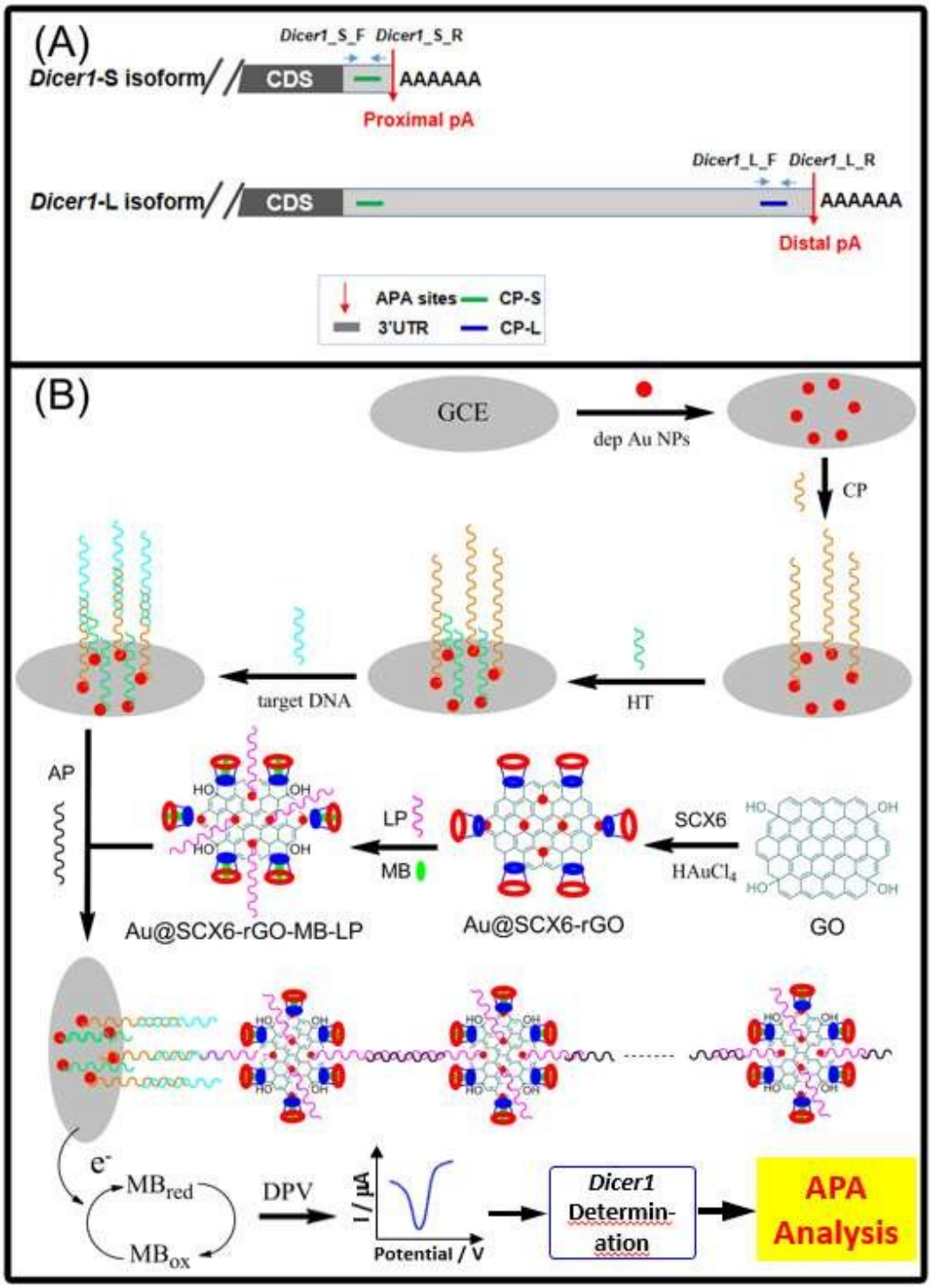

Scheme 1

Zhao et al.

View Article Online
DOI: 10.1039/C6NR09300K

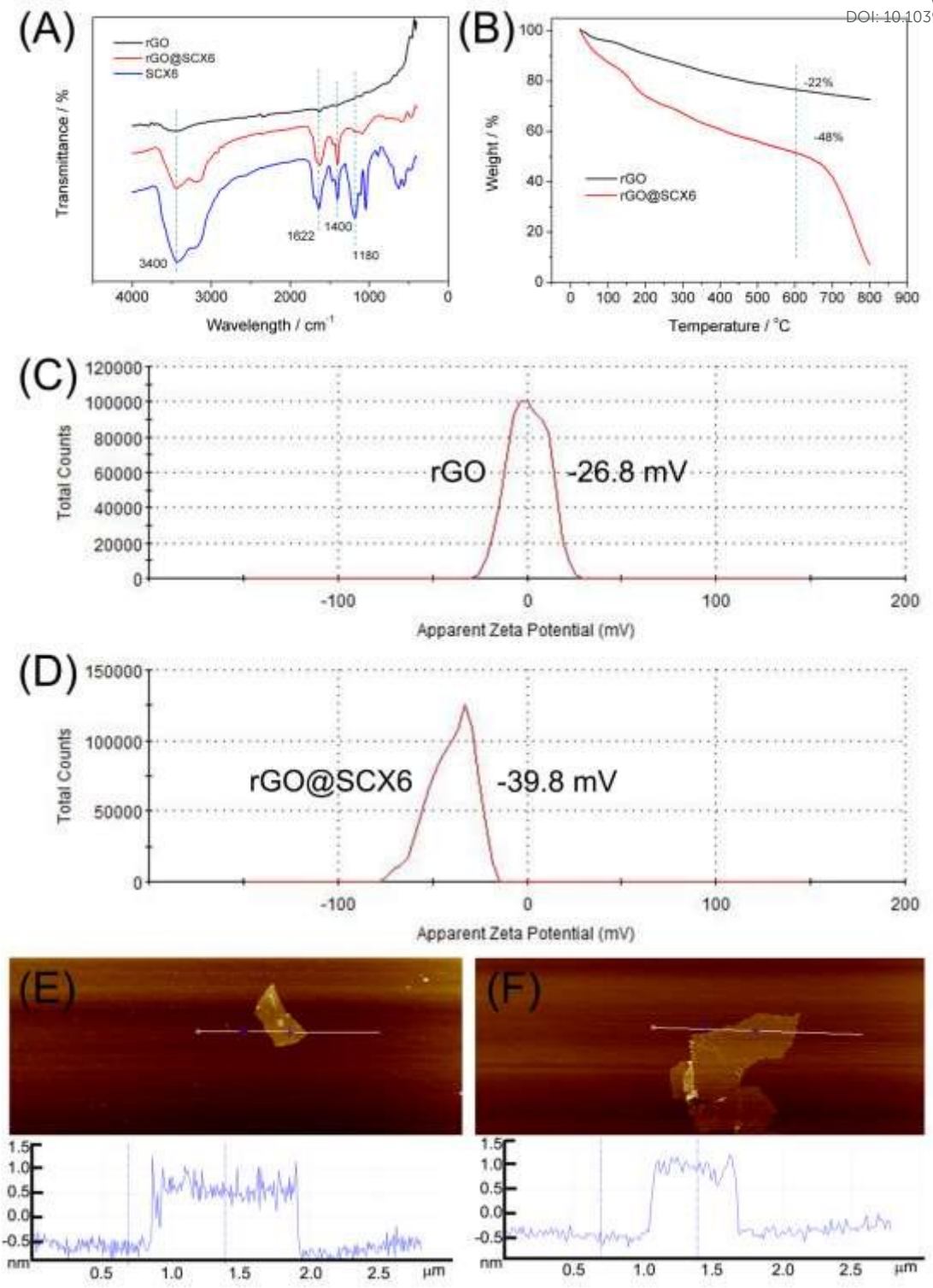

Fig. 1

Zhao et al.

View Article Online
DOI: 10.1039/C6NR09300K

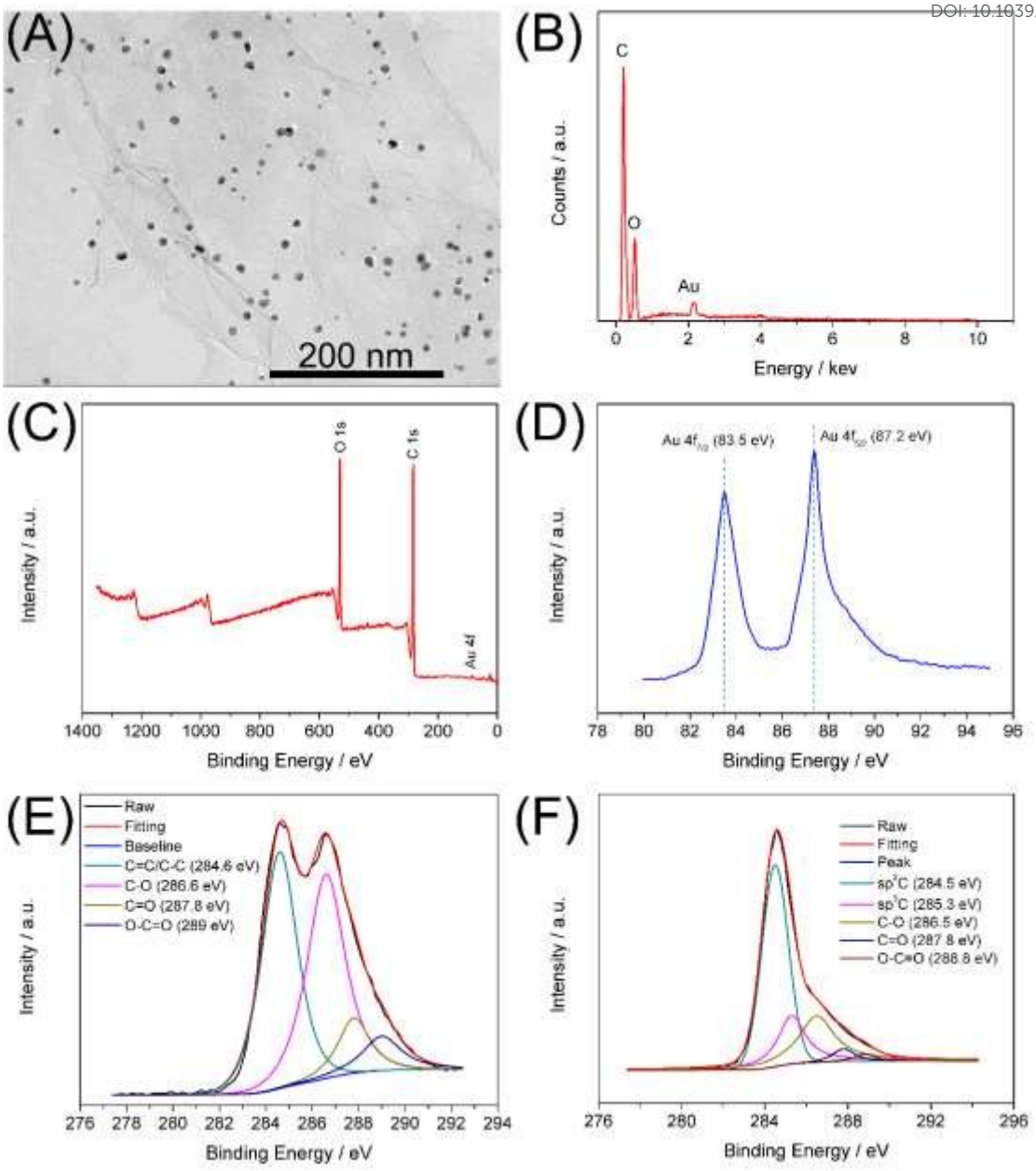

Fig. 2

Zhao et al.

View Article Online
DOI: 10.1039/C6NR09300K

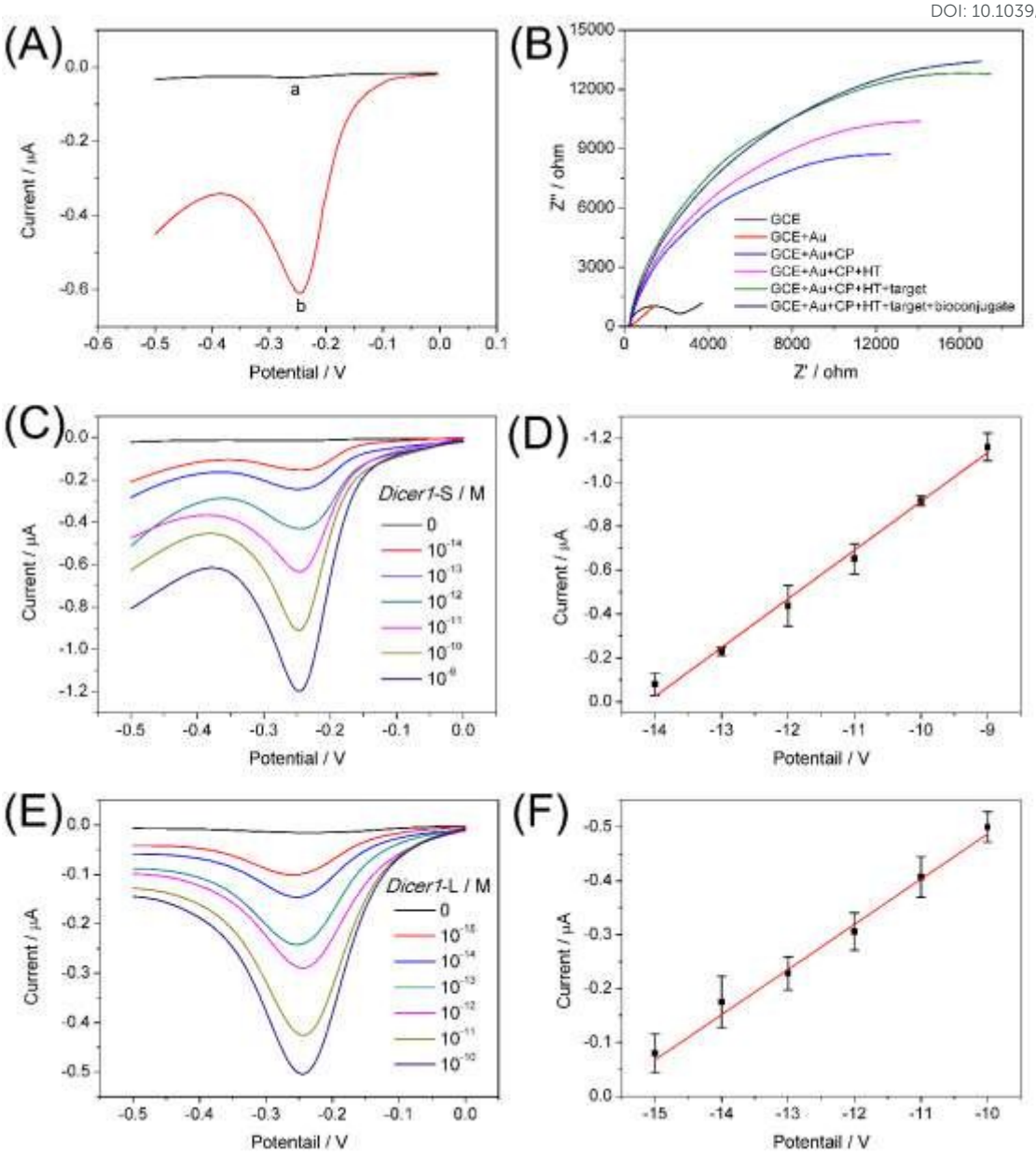

Fig. 3

Zhao et al.

View Article Online
DOI: 10.1039/C6NR09300K

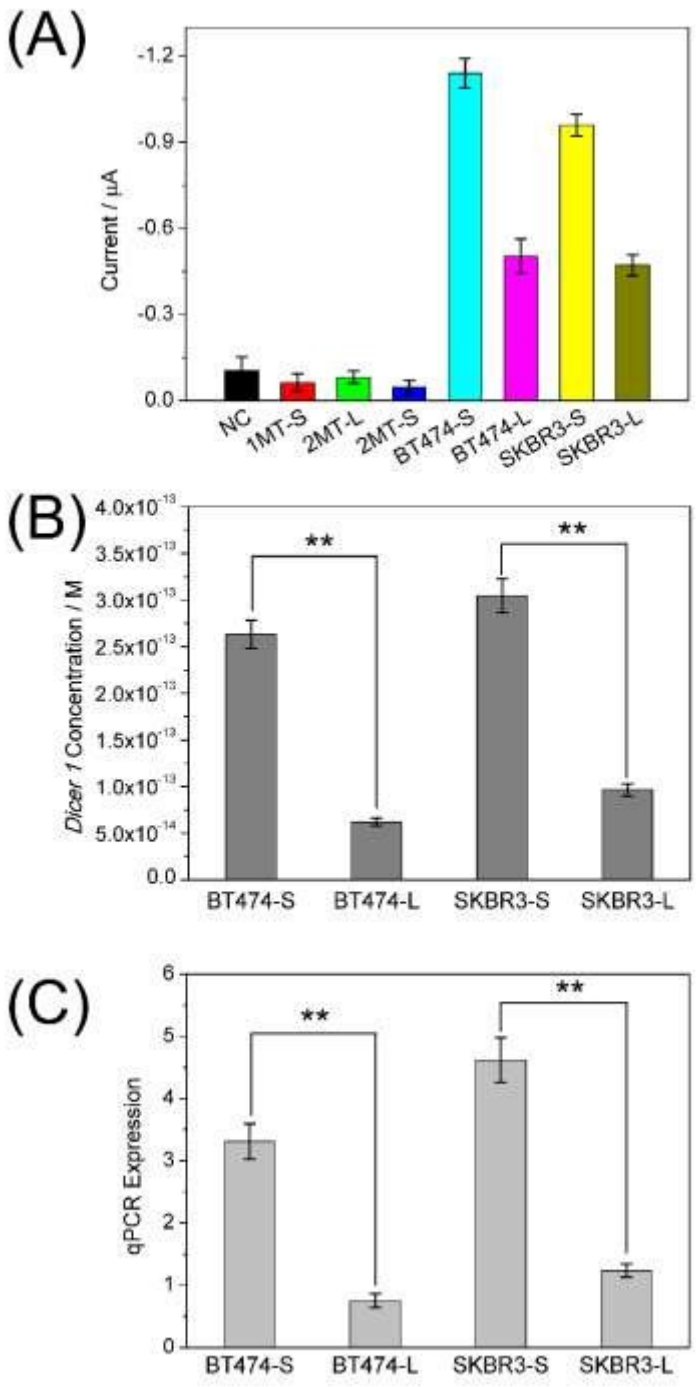

Fig. 4

Zhao et al.

View Article Online
DOI: 10.1039/C6NR09300K

Table 1

Comparison of the proposed biosensor with some previous published literatures for detection of 3'UTR.

Electrode or matrix	Sample	Method	Liner range (M)	LOD (fM)	Ref.
PtPd/GO/Au/HRP	non-coding RNA	DPV	10^{-12} - 10^{-6}	247	13
Au/graphene/HRP	microRNA-21	DPV	10^{-13} - $7*10^{-11}$	60	32
PDB film	Let-7c	EIS	$5*10^{-15}$ - 10^{-12}	2.0	37
Ferrocene/Au NPs	miRNA-182	DPV	10^{-14} - $2*10^{-12}$	10	38
Streptavidin-modified magnetic beads	miRNA-522	DPV	10^{-8} - $2*10^{-6}$	10^{6}	39
Star trigon structure and endonuclease based sensor	miRNA	SWV	10^{-16} - 10^{-9}	0.03	40
Au@SCX6-rGO-MB	*Dicer1*-S	DPV	10^{-14} - 10^{-9}	3.5	This work
Au@SCX6-rGO-MB	*Dicer1*-L	DPV	10^{-15} - 10^{-10}	0.53	This work

Table 1

Zhao et al.